

# First experimental evidence of one-dimensional plasma modes in superconducting thin wires

B. Camarota<sup>a</sup>, F. Parage<sup>a</sup>, F. Balestro<sup>a</sup>, P. Delsing<sup>b</sup> and  
O. Buisson<sup>a</sup>

<sup>a</sup> *Centre de Recherches sur les Très Basses Températures, Laboratoire Associé à l'Université Joseph Fourier, C.N.R.S., BP 166, 38042 Grenoble-Cédex 9, France.*

<sup>b</sup> *Department of Microelectronics and Nanoscience, Chalmers University of Technology and Goteborg University, S-412 96, Goteborg, Sweden.*

## Abstract

We have studied niobium superconducting thin wires deposited onto a SrTiO<sub>3</sub> substrate. By measuring the reflection coefficient of the wires, resonances are observed in the superconducting state in the 130 MHz to 4 GHz range. They are interpreted as standing wave resonances of one-dimensional plasma modes propagating along the superconducting wire. The experimental dispersion law,  $\omega$  versus  $q$ , presents a linear dependence over the entire wave vector range. The modes are softened as the temperature increases close the superconducting transition temperature. Very good agreement are observed between our data and the dispersion relation predicted by Kulik [1] and Mooij and Schön [2] .

PACS numbers: 72.15.Nj, 73.50.-h, 74.40.+k, 74.76.Db

Quantum phenomena in mesoscopic physics such as tunnelling effects, quantum fluctuations or decoherence processes are intimately related to the description of the environment. Its effects on quantum systems were extensively discussed in the last two decades. Dissipative environment was taken into account in the seminal Caldeira-Leggett study in order

to treat the macroscopic quantum tunneling in a tilted washboard potential [3]. Slightly afterwards quantum phase transition was predicted for Josephson junctions in the presence of a resistive environment [4].

In most of Josephson junctions experiments, the dissipative environment corresponds to external circuits made by the measurement circuit and is therefore extrinsic to the quantum system. In contrast in thin superconducting wires, the environment is intrinsic to the system. The related modes are the one-dimensional (1D) plasma modes propagating along the wire. They were predicted for the first time in a superconducting wire by Kulik [1] and later analysed by Mooij and Schön using non-equilibrium superconductivity model [2]. The restoring force is the long range Coulomb interaction. Because of the restricted geometry, the charge mode is not shifted to the bulk plasma frequency and has a sound like dispersion relation. Due to the gapless dispersion law of the environmental modes, quantum fluctuations in superconducting thin wires show critical behaviours [5–7]. A new quantum superconducting insulator phase transition has recently been predicted [8] and observed in ultra-thin nano-wires [7]. The driving parameter of the phase transition is the friction term coming from the interaction between the quantum system and the environmental modes.

In a thin superconducting loop closed by a Josephson junction, quantum fluctuations of the propagating plasma modes are predicted to renormalize the Josephson energy of the junction [9]. Furthermore these collective excitations are expected to modify IV characteristics of normal metal-superconductor tunnel junction [10,11]. In Josephson junction arrays the plasma modes, also called spin-waves, can affect the quantum dynamics of vortices [12–14].

Although many theoretical and experimental works have pointed out the importance of one-dimensional (1D) plasma modes in thin superconducting wires as environmental modes, no experiments have succeeded in observing them yet. Indeed up to now, to our knowledge, only two-dimensional plasma modes have been measured in superconducting granular aluminium films [15], later in YBCO films [21] and more recently in superconducting wires networks [17].

In this letter we report the first experimental evidence of propagating 1D-plasma modes in

superconducting wires. The wires were deposited onto strontium titanate (SrTiO<sub>3</sub>) crystal. The configuration "superconducting film/SrTiO<sub>3</sub>" was proven to be a *model experimental system* to study general properties of plasma modes [15,17]: in fact superconducting properties give a very weak damping of plasma oscillations, moreover the high dielectric constant of the SrTiO<sub>3</sub> ( $\epsilon_m \approx 10^4$  at low temperatures) reduces their energy by two orders of magnitude.

Three different wires, *A*, *B* and *C* were measured. Each one was deposited onto a (110) SrTiO<sub>3</sub> substrate of thickness  $H = 0.3$  mm. The wires were obtained from very thin niobium films of about 10 nm thickness evaporated in a ultrahigh vacuum chamber at room temperature. A 5 nm-thin layer of silicon was added in order to protect the niobium during the lithography process. The wire pattern was defined on a 130-200 nm thick negative Nover [18] resist layer by electron-beam lithography. Both silicon and niobium layers were etched in a SF<sub>6</sub> plasma. Next the Nover resist was removed by oxygen plasma leaving the niobium pattern. The dimension of the wires such as their width,  $W$ , thickness,  $t$ , and total length,  $L$ , are given in Table I. In order to perform electrical bonding, the wire is widened to a 30  $\mu\text{m}$  width over a 100  $\mu\text{m}$  length at its two extremities.

Table I summarizes the main geometrical parameters and physical properties of the three different measured wires. The critical temperature of the superconducting transition was obtained from transport measurements and taken at the midpoint of the resistive transition. The film resistivity  $\rho$  was measured just above the superconducting transition. The penetration depth  $\lambda_{\text{th}}(0)$  was derived from the BCS dirty model,  $\lambda_{\text{th}}(0) = \lambda_{\text{L}}(0)(\xi'_0/l)^{1/2}$  where  $\lambda_{\text{L}}(0) = 37$  nm is the London length,  $\xi'_0 = 62$  nm(9.25  $K/T_c$ ) the modified Pippard coherence length [19] and  $l$  the mean free path deduced from the resistivity by taking for niobium  $\rho l = 0.72 \cdot 10^{-5} \mu\Omega \cdot \text{cm}^2$ .

In order to observe plasma modes resonances, reflection coefficient measurements were performed in the 130 MHz to 4 GHz range using an HP8720B vector analyzer. A cryogenic 50 $\Omega$  coaxial cable guides the microwave between the vector analyser and the sample. The excitation of plasma modes is realized by injecting external charges into one extremity of the superconducting thin wire at the microwave frequency. The electrical contact between the

wire and the inner conductor of the coaxial line is made by means of a  $20\mu\text{m}$ -diameter aluminum bonding wire. The "superconducting wire/ $\text{SrTiO}_3$ " block is isolated from electrical ground plane by a thin teflon slab.

Since similar results have been obtained on the three different samples, only the sample *A* will be reported in detail. Typical reflection coefficient versus frequency is plotted in Fig. 1 between 130 MHz and 2 GHz. Resonances show two distinct behaviours. Above about 1.5 GHz, large resonant peaks are observed. They are weakly temperature dependent and exist both in the normal and the superconducting state. These resonances are related to dielectric modes inside the  $\text{SrTiO}_3$ . They appear above the cut frequency of the Transverse-Electric mode which is estimated at about 1.5 GHz for the configuration used in this experiment. Much more interesting are the resonances which appear below 1.5 GHz. Their amplitude and frequency are strongly temperature dependent. As the temperature increases, their peaks shift towards lower frequency, their amplitude decreases and their width increases. In the normal state, these resonances disappear.

Only two possible modes could explain the resonances below 1.5 GHz : the Transverse Electro-Magnetic (TEM) modes and the 1D plasma modes. Confusion between these two modes could be made because they both verify similar properties such as a quasi-linear dispersion law and a temperature dependence related to the superfluid density. However fundamental differences exist between them. Plasma modes need only one wire to propagate while TEM modes need the wire and a ground plane. The quasi-linear dispersion of 1D plasma modes comes from the long range Coulomb interaction of the wire whereas the linear dispersion of the TEM modes is explained by the short range Coulomb interaction of the wire screened by the ground plane. The following analysis of the experimental configuration can explain why TEM modes can not be taken into account to interpret our experimental results.

The superconducting wire/ $\text{SrTiO}_3$ /teflon slab/ground plane structure [22] corresponds to a microstrip whose the inner conductor is the wire and is separated from the ground plane by  $\text{SrTiO}_3$  and teflon slab dielectrics. The TEM mode related to this structure is

determined by the unit-length inductance,  $L_l$ , and capacitance,  $C_l$  [23]. The capacitance corresponds to the capacitance between the wire and the ground plane through the two dielectrics. By measuring the impedance of the wire at 130 MHz using the network analyser, the capacitance could be deduced,  $C_l \approx 0.45$  nF/m. Since the wire is superconducting, the inductance  $L_l$  is the sum of two terms: one is related to the kinetic inductance, estimated at about  $L_K \approx 5.2 \mu\text{H}/\text{m}$  for a penetration depth of about  $0.5 \mu\text{m}$ ; the other is related to the magnetic inductance of the microstrip ( $L_m \approx 1.3 \mu\text{H}/\text{m}$ ) [23]. For such parameters, the phase velocity of the TEM modes, given by  $1/\sqrt{L_l C_l}$ , is roughly  $2 \cdot 10^7$  m/s. Thus, the first resonance related to the TEM mode propagating along the wire is expected at about 4 GHz, one order of magnitude higher than the observed ones. Therefore standing wave resonances of TEM modes can not explain the resonances measured below 1.5 GHz.

Hence we will discuss the observed resonances as standing wave resonances of 1D plasma modes. Indeed as it was already shown in a previous study [15], the wave vectors associated to plasma resonances obey the  $qL = n\pi$  selection rule for standing waves, where  $n$  an integer indexing the different resonances. An experimental  $\omega$  vs.  $q$  plasma dispersion relation is therefore obtained. Fig. 2 presents the dispersion law of sample A for different temperatures. The linear dependence of the dispersion relation is observed over the entire wave vector range and for temperatures going from 1.5 K to very close to  $T_c$ . As the temperature increases, the modes are strongly softened. The mode velocity varies from  $2 \cdot 10^5$  m/s near  $T_c$  up to  $1.5 \cdot 10^6$  m/s at low temperature, but is always slower than the light velocity in the SrTiO<sub>3</sub>. Above  $T_c$ , no dispersion curve exists because of the disappearance of the resonances.

Theoretical studies on plasma modes in superconducting wires [1,2] predict a quasi-linear dispersion relation if the radius  $r_0$  of the wire is much thinner than the penetration depth,  $\lambda(T)$ , and the wavelength ( $r_0 \ll \lambda(T)$  and  $qr_0 \ll 1$ ). Plasma modes dispersion relation is then given by:

$$\omega_p^2 = \frac{r_0^2}{\epsilon_0 \mu_0 \epsilon_m \lambda^2(T)} \tilde{q}^2 \ln(1/(\tilde{q}r_0)) \quad (1)$$

where  $\tilde{q} = \sqrt{q^2 - \mu_0 \epsilon_0 \epsilon_m \omega_p^2}$  is the parameter characterizing evanescent length inside the

dielectric, taking into account retardation effects. Such theoretical results were obtained for a cylindrical shaped wire embedded in an infinite isotropic medium of dielectric constant  $\epsilon_m$ .

The experimental configuration presented here shows some important differences with the one considered in the theoretical derivations. Indeed the SrTiO<sub>3</sub> is finite size and a ground plane is present close to the superconducting wire. One-dimensional plasma modes are very sensitive to the finite dimension of the sample because of the long range Coulomb interaction which extends up to few millimeters if very low energy plasma modes are considered. Their propagation may thus be expected to be strongly modified.

In order to take into account these perturbations we have derived, in a previous work [22], the plasma modes dispersion relation of a wire in the real experimental configuration. Two simplifications were applied. Firstly the SrTiO<sub>3</sub> dielectric constant was assumed isotropic with an average value  $\epsilon_m = (\epsilon_{001}\epsilon_{110}\epsilon_{1\bar{1}0})^{1/3}$ . Secondly the rectangular wire was approximated by a cylindrical wire of radius  $r_0$  with cross section  $\pi r_0^2/2 = Wt$  and half-immersed in the semi-space occupied by the SrTiO<sub>3</sub>. Because of the very high dielectric constant of SrTiO<sub>3</sub> ( $\epsilon_m \approx 12500$  for sample A), it was possible to take into account the finite size of the experimental configuration. As a result the derived dispersion relation of our sample configuration [22] was proven to be well described by the predicted 1D plasma modes one, Eq. 1, as long as the evanescent length is smaller than twice the SrTiO<sub>3</sub> thickness ( $2\tilde{q}H > 1$ ). This allowed us to conclude that the experimental set-up represents an optimal configuration for the study of plasma modes in superconducting wires.

The comparison between the experimental dispersion law and the theoretical one given by Eq. 1 is shown in Fig. 2. The theoretical quasi-linear 1D plasma mode dispersion fits very well the experimental one for all the temperatures and over the entire wave vector range. In the range of wave vectors accessible by this experiment, the logarithmic deviation predicted by the theory is not observed. Since  $\epsilon_m$  is measured independently using the dielectric resonances [20],  $\lambda(T)$  is the only free parameter. The experimental penetration depth extracted from the fit versus the reduced temperature  $T/T_c$  is plotted in Fig. 3 for the

three different samples. We notice that the required condition  $2\tilde{q}H > 1$  is fulfilled for sample A and B over all the temperature range but not for sample C below 8 K justifying that the penetration depth of sample C is plotted only near  $T_c$ . As the temperature increases close to  $T_c$ , the penetration depth diverges. At low temperature ( $T/T_c < 0.5$ ),  $\lambda(T)$  saturates. The temperature dependence cannot be well fitted by the Gorter-Casimir law but by an equivalent one:  $\lambda(T) = \lambda_{exp}(0)/\sqrt{1 - (T/T_c)^2}$  where  $\lambda_{exp}(0)$  is the only free parameter. The same temperature dependence has also been found in previous studies on niobium wire networks [17,20]. The penetration depths at  $T=0$  K obtained from the fit,  $\lambda_{exp}(0)$ , are summarized in Table I for the three samples. These experimental values are consistent with the penetration depth derived using the BCS dirty limit.

In conclusion one-dimensional plasma modes have been observed for the first time by measuring the reflection coefficient of thin niobium wires. By using a very high dielectric constant substrate, the stontium titanate, the long range Coulomb interaction is strongly weakened, reducing by two orders of magnitude the plasma modes energy. A dispersion law has been obtained which shows a linear dependence. Moreover the plasma modes are softened as the temperature increases close to the superconducting transition temperature. Both the dispersion law and the temperature dependence are well explained by the predicted plasma modes dispersion given by Eq. 1.

## ACKNOWLEDGMENTS

We thank M. Doria, G. Falci and F.W.J Hekking for invaluable discussions. This research is supported by european Union under TMR Program "Dynamics of nanofabricated superconducting circuits".

## REFERENCES

- [1] I.O. Kulik, *Sov. Phys.-JETP* **38**, 1008 (1974).
- [2] J.E. Mooij and G. Schön, *Phys. Rev. Lett.* **55**, 114 (1985).
- [3] A.O. Caldeira and A.J. Leggett, *Phys. Rev. Lett.* **46**, 211 (1981).
- [4] A. Schmid, *Phys. Rev. Lett.* **51**, 1506 (1983).
- [5] N. Giordano, *Phys. Rev. Lett.* **61**, 2137 (1988).
- [6] J.M. Duan, *Phys. Rev. Lett.* **74**, 5128 (1995).
- [7] A. Bezryadin, C.N. Lau and M. Tinkham, *Nature* **404**, 971 (2000).
- [8] A.D. Zaikin, D.S. Golubev, A. van Otterlo and G.T. Zimanyi, *Phys. Rev. Lett.* **78**, 1552 (1997).
- [9] F.W.J. Hekking and L.I. Glazman, *Phys. Rev. B* **55**, 6551 (1997).
- [10] Y.B. Kim and X.G. Wen, *Phys. Rev. B* **48**, 6319 (1993).
- [11] P. Falci, R. Fazio, A. Tagliacozzo and G. Giaquinta, *Europhys. Lett.* **30**, 169 (1995).
- [12] U. Eckern and A. Schmid, *Phys. Rev. B* **39**, 6441 (1989).
- [13] H. van der Zant, F.C. Fritschy, T.P. Orlando and J.E. Mooij, *Phys. Rev. B* **47**, 295 (1993).
- [14] R. Fazio, A. van Otterlo and G. Schön, *Europhys. Lett.* **25**, 453 (1994).
- [15] O. Buisson, P. Xavier, and J. Richard, *Phys. Rev. Lett.* **73**, 3153 (1994); *Phys. Rev. Lett.* **74E**, 1493 (1995).
- [16] F.J. Dunmore, D.Z. Liu, H.D. Drew, and S. Das Sarma, *Phys. Rev. B* **52**, R731 (1995).
- [17] F. Parage, M.M. Doria and O. Buisson, *Phys. Rev. B - Rapid Comm.* (October 1998).



- [18] Nover: Raith Gmbh, Hauert 18, Technologiepark, D44227 Dortmund, Germany.
- [19] J. Halbritter, *Z. Phys.* **266**, 209 (1974).
- [20] F. Parage. *PhD thesis* (1997).
- [21] F.J. Dunmore, D.Z. Liu, H.D. Drew, and S. Das Sarma, *Phys. Rev. B* **52**, R731 (1995)..
- [22] B. Camarota, F. Parage, I. Wooldridge, P. Delsing and O. Buisson, *J. Low temp. Phys.* **118**, 589 (2000).
- [23] *Microstrip lines and slotlines*, K.C. Gupta, Ramesh Garg and I.J. Bahl, Artech House, INC. (1979).

TABLES

TABLE I. Characteristics of the different niobium wires.

Samples	$t$ (nm)	$W$ ( $\mu\text{m}$ )	$L$ (mm)	$T_c$ (K)	$\rho$ ( $\mu\Omega\cdot\text{cm}$ )	$l$ (nm)	$\xi'_0$ (nm)	$\lambda_{\text{th}}(0)$ ( $\mu\text{m}$ )	$\lambda_{\text{exp}}(0)$ ( $\mu\text{m}$ )
A	12	5.0	2.2	5.19	55	1.3	110	0.34	0.50
B	11	3.0	2.25	6.68	32.4	2.2	86	0.23	0.21
C	10	6.0	2.38	8.84	16.8	4.3	65	0.14	0.14

FIGURES

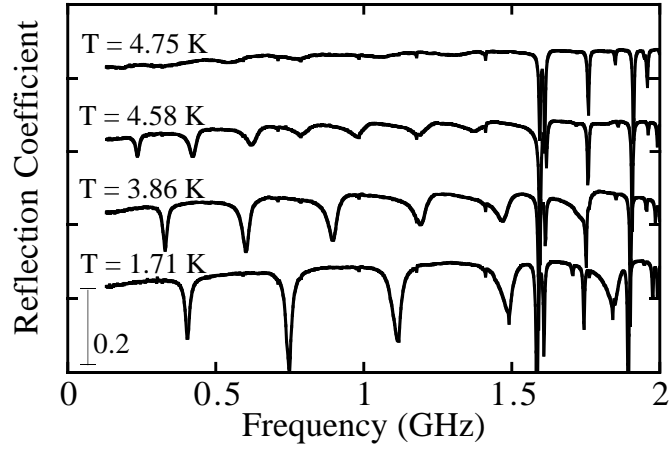


**Fig.1.** Reflection coefficient versus frequency at different temperatures. A vertical shift of the different curves have been introduced for clarity.

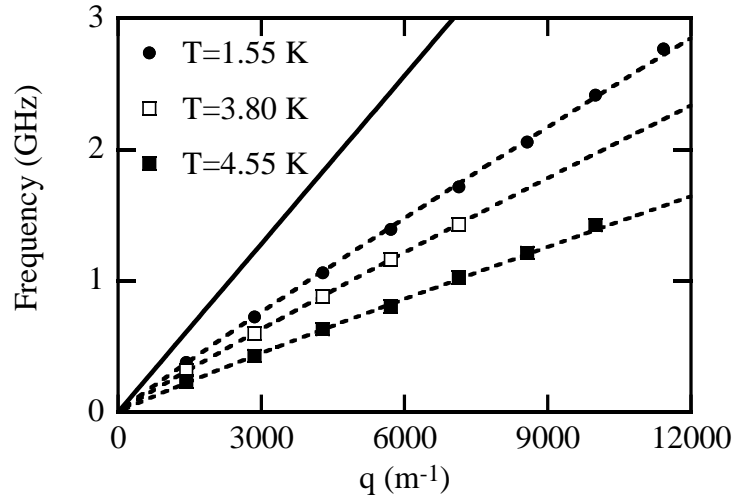


**Fig.2.** Dispersion relation of sample A measured at three different temperatures (points) and fitted by the theoretical dispersion law given by Eq. 1 (dashed lines). Light dispersion inside the  $\text{SrTiO}_3$  (continuous line) is plotted for comparison.

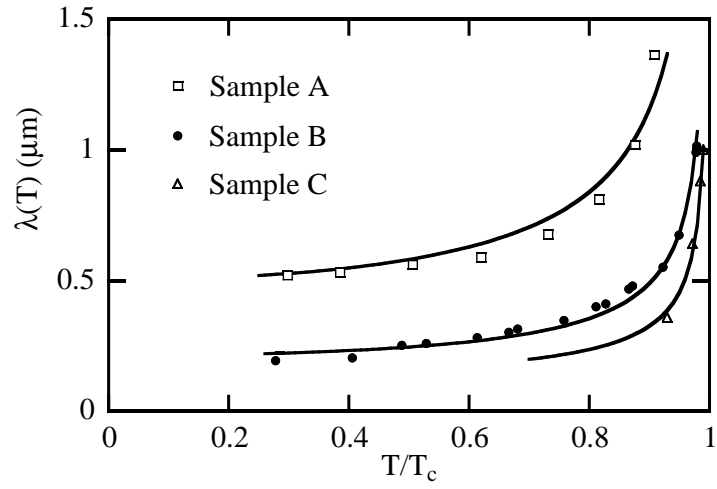


**FIG. 3.** Experimental penetration depth (dots) deduced from the fit of Eq.1 as a function of the reduced temperature  $T/T_c$ . Solid lines are obtained from  $\lambda(T) = \lambda_{exp}(0)/\sqrt{1 - (T/T_c)^2}$  with  $\lambda_{exp}(0)$  as adjustable parameter (see values in Table I).